Available online at www.sciencedirect.com
ScienceDirect
Physica E 40 (2008) 1844–1847
PHYSICA E
www.elsevier.com/locate/physe

# Frequency-selective single-photon detection with a double quantum dot

R. Leturcq[a,*], S. Gustavsson[a], M. Studer[a], T. Ihn[a], K. Ensslin[a], D.C. Driscoll[b], A.C. Gossard[b]

[a]*Laboratory for Solid State Physics, ETH Zurich, 8093 Zurich, Switzerland*
[b]*Materials Department, University of California, Santa Barbara, CA 93106, USA*

Available online 4 December 2007

**Abstract**

We use time-resolved charge detection methods to detect single photons absorbed by a double quantum dot (DQD). With the ability to tune the energy levels in the DQD, the frequency of the detected photon can be continuously varied between 10 and 80 GHz. The working principle of this device is demonstrated by measuring the radiation emitted by a nearby quantum point contact driven out-of-equilibrium at large bias voltage.


*PACS:* 73.23.Hk; 72.30.+q; 72.70.+m

*Keywords:* Semiconductor quantum dots; Single charge detection; Photon-assisted tunneling; Shot noise

Similar to real atoms and molecules, single and double quantum dots (DQDs) can absorb light through electronic transitions. There are, however, two main differences between atoms and quantum dots. The first is the frequency range of the absorbed photons, which is in the microwave range for typical excited states in quantum dots realized in GaAs as compared to visible light for atomic excitations. The second is the possibility to tune the electronic properties of these artificial atoms and molecules, and to integrate them in more complex circuits, which make them interesting for building very sensitive detectors in the microwave range. Such detectors could be of great importance in order to study the radiation emitted by quantum conductors [1].

A DQD has already been proposed as a microwave photon detector [2], with a great advantage due to the possibility to tune the detected frequency by changing the energy levels in both dots using simple gates. However, such a scheme has not been realized experimentally, in particular due to the small current expected to be measured. In parallel, time resolved detection of single electrons using a quantum point contact (QPC) read-out [3,4] has shown the possibility to measure single-electron transport through quantum dots, with a current resolution well below any conventional electronics [5,6]. Here we combine both techniques, photon-assisted tunneling through a DQD and time-resolved detection of single-charge tunneling, in order to resolve the absorption of single photons by the DQD detector. With this frequency-tunable single-photon detector in the microwave range, we study photons emitted by a quantum conductor, which in this case is a QPC driven out-of-equilibrium by a bias voltage $V_{\mathrm{bias,QPC}}$.

The sample shown in Fig. 1(a) has been fabricated by local oxidation of a GaAs/AlGaAs heterostructure using the tip of an atomic force microscope [7]. It consists of two dots in series [dashed circles in Fig. 1(a)], electrostatically coupled to a QPC. We set the QPC conductance such that the current through the QPC is directly related to the occupation number in the DQD [8]. The current through the QPC is recorded as a function of time with a time resolution of 30 μs. The measurements have been done in a $^3$He/$^4$He dilution refrigerator at an electronic temperature of 100 mK.

In the regime depicted in Fig. 1(b), the current through the DQD is suppressed due to Coulomb blockade [step I]. However, the absorption of a photon can excite the electron trapped in the left dot into the right dot [step II]. In our case, the tunneling rate $\Gamma_D$ for the electron to leave

*Corresponding author. Tel.: +41 446 332316; fax: +41 446 331146.
*E-mail address:* leturcq@phys.ethz.ch (R. Leturcq).

1386-9477/$ - see front matter 
doi:10.1016/j.physe.2007.11.032

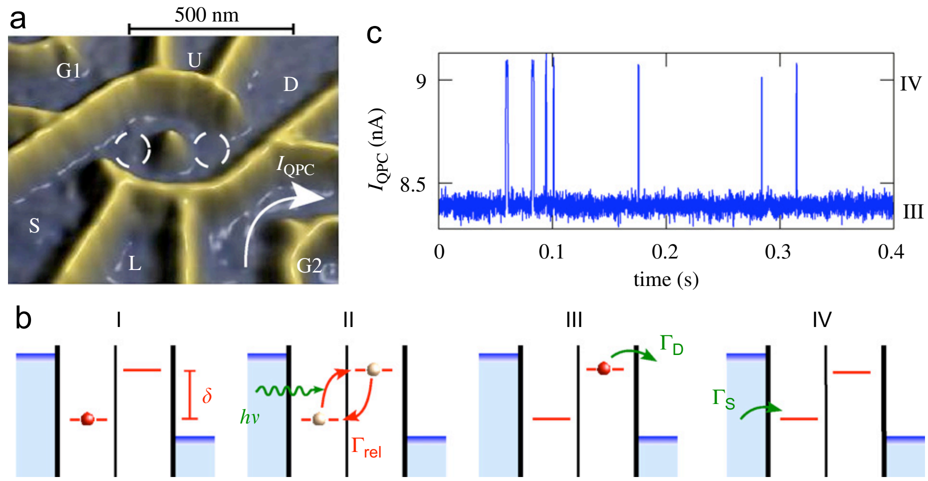


Fig. 1. (a) Picture of the double quantum dot device coupled to the quantum point contact. The yellow lines are oxide lines defining electrically isolated regions in the two-dimensional electron gas beneath. The two dots (dashed circles) are coupled in series and connected to source (S) and drain (D) contacts. The gates U, L, G1 and G2 allow to tune respectively the interdot tunnel barrier and the occupation number in each dot. (b) Scheme of the double dot occupation in the configuration for detecting single photons. (c) Current in the quantum point contact measured as a function of time in the regime depicted in (b). While states I–III correspond to the same occupation number and therefore give the same current level, state IV results in a larger current level, which allows to detect the absorption of a single photon as a spike in $I_{QPC}$.

the right dot is chosen to be small compared to the relaxation rate $\Gamma_{rel}$, and the electron will experience a fast cycle of absorption–relaxation processes. However, there is a finite probability given by $\Gamma_D/\Gamma_{rel}$ for the electron to leave the right dot [step III], which concludes the absorption–relaxation cycle before an electron enters the left dot [step IV]. This step is chosen to be slow enough (through the choice of $\Gamma_D$) in order to be detected with the finite bandwidth detector.

In order to measure single-charge tunneling through the DQD, the tunneling rates to the leads are tuned to a low value, typically 1 kHz, in order to keep it lower than the bandwidth of the charge detector (10 kHz). The interdot tunnel coupling is tuned to a large value, a few GHz. In this configuration, only the events corresponding to an electron leaving the dot [step III] and the next electron entering the dot [step IV] can be detected, and interdot transitions are not resolved. This is in contrast to the experiment of Fujisawa et al., for which the interdot tunneling is also slow, and can be detected [6]. In our case, a typical time trace of the current through the QPC shown in Fig. 1(c) has two values, a low value corresponding to one excess electron in the DQD [steps I–III], and a larger value corresponding to zero excess electron in the DQD [step IV]. Each spike in Fig. 1(c) can then be attributed to the absorption of a photon directly followed by an electron leaving the DQD. In the following we count the number of spikes in a given time interval, which is directly proportional to the total number of photons absorbed by the DQD [9].

In order to tune our device into the correct regime, we have measured the charge stability diagram as shown in Fig. 2. In this diagram, counts are expected in triangular regions, for which the levels in both quantum dots are

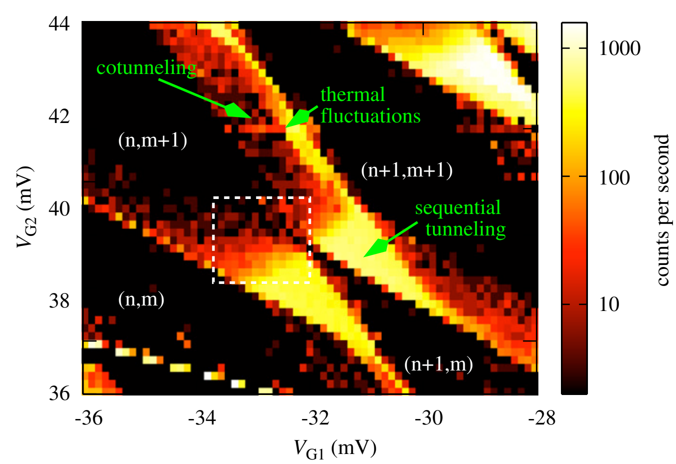


Fig. 2. Charge stability diagram of the double quantum dot measured by counting electrons. A finite bias voltage is applied through the double dot, which gives characteristics triangles. The number of electrons in each dot is indicated in brackets. The dashed square is the region of interest for observing photon assisted tunneling, for which a zoom is shown in Fig. 3.

within the bias voltage window, and sequential tunneling is allowed [10]. Due to the large interdot coupling, we also observe faint bands joining the triangles, which can be attributed to cotunneling though one of the dots [12]. With our charge detection setup, we also see narrow lines connecting the edges of the triangles, which correspond to thermal fluctuations of charge between one of the quantum dot and the nearby lead [9]. The interesting regions for observing events due to photon absorption are outside these two understood regions, and is known as photon-assisted tunneling regime [10].

One of these interesting regions of photon-assisted tunneling is enlarged in Fig. 3, and emphasized in

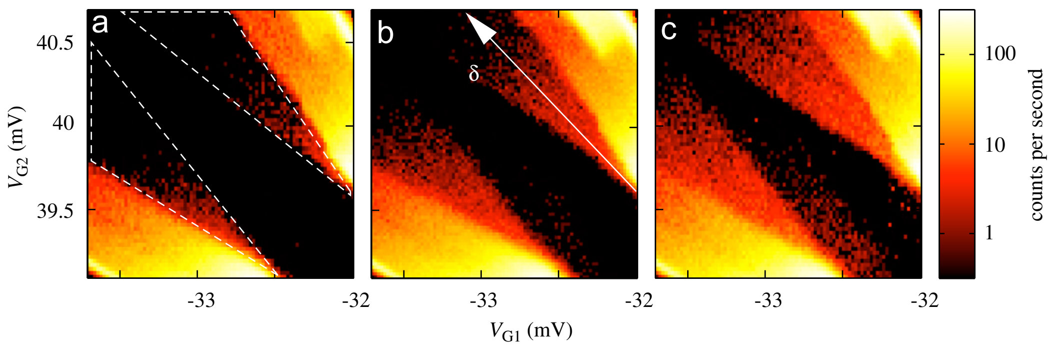


Fig. 3. Close-up of the double dot stability diagram close to the degeneracy points, corresponding to the dashed square in Fig. 2, for different bias voltages applied to the QPC: (a) $V_{\mathrm{bias,QPC}} = 200\,\mu\mathrm{V}$, (b) $V_{\mathrm{bias,QPC}} = 300\,\mu\mathrm{V}$ and (c) $V_{\mathrm{bias,QPC}} = 400\,\mu\mathrm{V}$. In (a), the lower triangular dashed line represent the region depicted in Fig. 1(b), for which tunneling is suppressed without photon absorption. A similar region in the upper part is the corresponding regime, but involving tunneling of a hole instead of an electron. In (b), the arrow shows the line along which the energy between the levels in both dots (detuning $\delta$) is changed.

Fig. 3(a) by dashed triangles. The lower triangle corresponds to the scheme described in Fig. 1(b), involving tunneling out and in of an electron. The upper triangle corresponds to the case where both levels are below the chemical potential of the leads. In this case, a process similar to Fig. 1(b), but with tunneling *out and in* of a hole (or, equivalently, tunneling *in and out* of an electron) [10]. Since both, electron or hole processes are equivalent, results from both cases are presented here without distinction, with the same labellings for the rate of an electron (hole) tunneling into the DQD, $\Gamma^{\mathrm{e}}_{\mathrm{in}} \equiv \Gamma^{\mathrm{h}}_{\mathrm{in}} \equiv \Gamma_{\mathrm{in}}$, and out of the DQD, $\Gamma^{\mathrm{e}}_{\mathrm{out}} \equiv \Gamma^{\mathrm{h}}_{\mathrm{out}} \equiv \Gamma_{\mathrm{out}}$.

Figs. 3(b) and (c) show the same region as in Fig. 3(a), but for higher bias voltage applied on the QPC detector. Interestingly, only the counts in the triangular regions marked by dashed lines in Fig. 3(a) are significantly affected by the increase of the QPC bias, while the regions of sequential tunneling, cotunneling and thermal fluctuations are not. We conclude that photon-assisted tunneling is generated by photons emitted from the nearby QPC. The energy transfer between the QPC and the QD could also be driven through phonons [11] or plasmons. However, a detailed comparison with the theory presented below indicates that photons are the most probable origin [9].

Indeed, it is well known that a QPC driven out-of-equilibrium acts as a photon source with broad-band spectrum in the microwave range [1]. The shot noise in the QPC induces high frequency potential fluctuations which can be detected as microwave photons by our detector. While few other experiments have measured the high-frequency noise of a QPC using either photon-assisted tunneling through a single quantum dot [13] or a highly sensitive microwave detection scheme [14], our method allows single-photon detection. In addition, the frequency detected in our device is given by the energy spacing between the levels in both quantum dots, the detuning $\delta$ [see Fig. 1(b)], which can be continuously and easily tuned by changing the voltages applied to gates G1 and G2. Such a detuning line which allows to vary the frequency of our detector is shown by the arrow in Fig. 3(b).

In order to characterize further our frequency-tunable single photon detector, we have studied the rate of photon emission by the QPC as a function of the bias voltage $V_{\mathrm{bias,QPC}}$ applied across the QPC. The photon emission rate has been calculated in Ref. [2], and it decreases as a function of frequency up to a cut-off frequency $\nu = eV_{\mathrm{bias,QPC}}/h$. This decrease and cut-off are qualitatively seen in Fig. 3 along the $\delta$-axis, where the increase of the cut-off frequency with increasing $V_{\mathrm{bias,QPC}}$ is well seen as a shift of the $\delta$-value, where the number of counts vanishes. A quantitative analysis shows that the experimental data are very well fitted by the results of the theoretical calculations [9].

Until now we have been interested in counting the number of events which correspond to photon absorption. We now focus on the analysis of tunneling times into and out of the DQD, which have been shown to reveal additional information in the case of a single quantum dot [15]. From the time-trace of the current through the QPC shown in Fig. 1(c), we can calculate the average time spent in the low current level, which corresponds to the waiting time before the charge leaves the dot, and so to the rate $\Gamma_{\mathrm{out}}$ [15]. In the same way, the average time spent in the higher current level corresponds to the waiting time before the next charge enters the DQD, and so to the rate $\Gamma_{\mathrm{in}}$. These rates for hole transport, determined for a wider range of detuning $\delta$ and bias voltage applied to the QPC are shown in Fig. 4.

In the scheme shown in Fig. 1(b), it is expected that only the rate for a charge leaving the DQD depends on the absorption of a photon. The out-going rate should only depend on the tunnel barrier separating the right dot to the drain lead. This model is confirmed by Fig. 4, since only $\Gamma_{\mathrm{out}}$ depends on the detuning, while $\Gamma_{\mathrm{in}}$ keeps a constant value, until the detuning exceeds the energy of photons emitted by the QPC [left of the straight dashed line in Fig. 4(b)].

In this experiment, we demonstrate single-photon detection with a tunable frequency typically between 10 and 80 GHz. The low frequency limit is due to the interdot

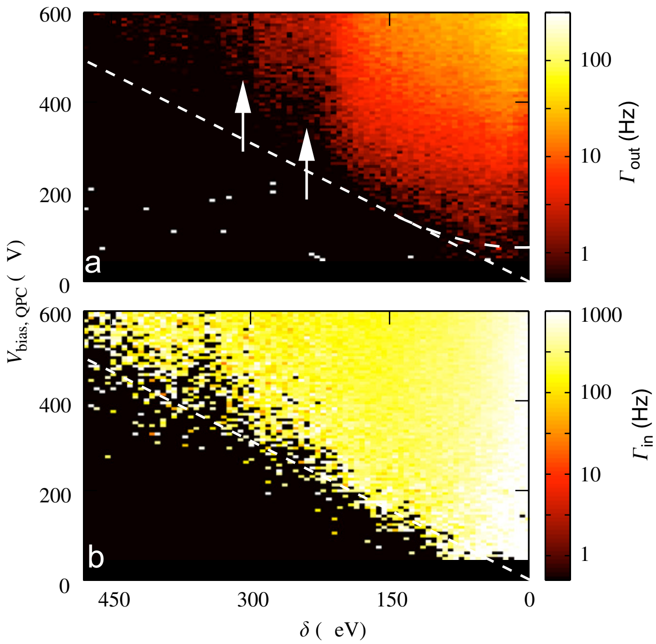


Fig. 4. Tunneling rates for (a) holes tunneling out of the DQD, $\Gamma_{out}$, and (b) holes tunneling into the DQD, $\Gamma_{in}$. These rates are calculated by averaging the waiting time respectively in the low current level, $\Gamma_{out} = 1/\langle\tau_{low}\rangle$, and in the high current level, $\Gamma_{in} = 1/\langle\tau_{high}\rangle$ [see Fig. 1(c)]. The straight dashed line correspond to the limit $\nu = eV_{bias,QPC}/h$, and the curved dashed line in (a) emphasizes the low frequency limit [see text].

tunnel coupling $t = 32\,\mu eV$, which hybridizes left and right dot states into bonding and anti-bonding states with a minimum energy spacing given by $2t$. This explains the drop of the count rate for $V_{bias,QPC} < 100\,\mu eV$ in the lower right part of Fig. 4(a), below the curved dashed line. The opposite high frequency limit is given by electronic excitations in individual quantum dots, with a typical energy scale $\Delta E \approx 200\,\mu eV$. At higher energy, intradot transitions will add to the original interdot process, which could explain the rapid drop of the count rates at large QPC bias voltage [see arrows in Fig. 4(a)].

Finally, an interesting quantity is the efficiency of our detector, which is given by the ratio $\Gamma_D/\Gamma_{rel}$. It is lower than $10^{-5}$ in our experiment, and it is limited by the low bandwidth of the detector and the fast relaxation. Using a faster detection scheme could provide a way to reach better efficiency. However, it was argued in Ref. [16] that such a scheme will not be able to give any statistical information on the photon emission, since the measured statistics will always be limited by the sub-Poissonian statistics of electrons tunneling through the DQD. For this purpose, it was proposed in the same reference to use several detectors in order to realize a correlation measurement. This scheme could be realized with two or more single-photon detectors.

In conclusion, we have shown that a DQD coupled to a QPC used as a single-charge detector can detect single photons with a tunable frequency in the microwave frequency range. This on-chip detection has been used to measure the high frequency shot noise spectrum of a QPC, and shows the expected linear dependence of the noise vs. frequency [9]. In the future, coupling several DQD detectors would be a way to measure non-classical statistics of photons emitted by a quantum conductor [16].

## References

[1] C.W.J. Beenakker, H. Schomerus, Phys. Rev. Lett. 86 (2001) 700.
[2] R. Aguado, L.P. Kouwenhoven, Phys. Rev. Lett. 84 (2000) 1986.
[3] R. Schleser, et al., Appl. Phys. Lett. 85 (2004) 2005.
[4] L.M.K. Vandersypen, et al., Appl. Phys. Lett. 85 (2004) 4394.
[5] S. Gustavsson, et al., Phys. Rev. Lett. 96 (2006) 076605.
[6] T. Fujisawa, T. Hayashi, R. Tomita, Y. Hirayama, Science 312 (2006) 1634.
[7] A. Fuhrer, et al., Superl. Microstruc. 31 (2002) 19.
[8] M. Field, et al., Phys. Rev. Lett. 70 (1993) 1311.
[9] S. Gustavsson, et al., Phys. Rev. Lett. 99 (2007) 206804.
[10] W.G. van der Wiel, et al., Rev. Mod. Phys. 75 (2003) 1.
[11] V.S. Khrapai, et al., Phys. Rev. Lett. 97 (2006) 176803.
[12] S. Gustavsson, et al., unpublished.
[13] E. Onac, et al., Phys. Rev. Lett. 96 (2006) 176601.
[14] E. Zakka-Bajjani, et al., arXiv:0704.0907.
[15] S. Gustavsson, et al., Phys. Rev. B 74 (2006) 195305.
[16] C.W.J. Beenakker, H. Schomerus, Phys. Rev. Lett. 93 (2004) 096801.